

Figure S1. Knockdown of GSK-3 α attenuates high-fat diet (HFD)-induced lipotoxic cardiomyopathy, Related to Figure 1.

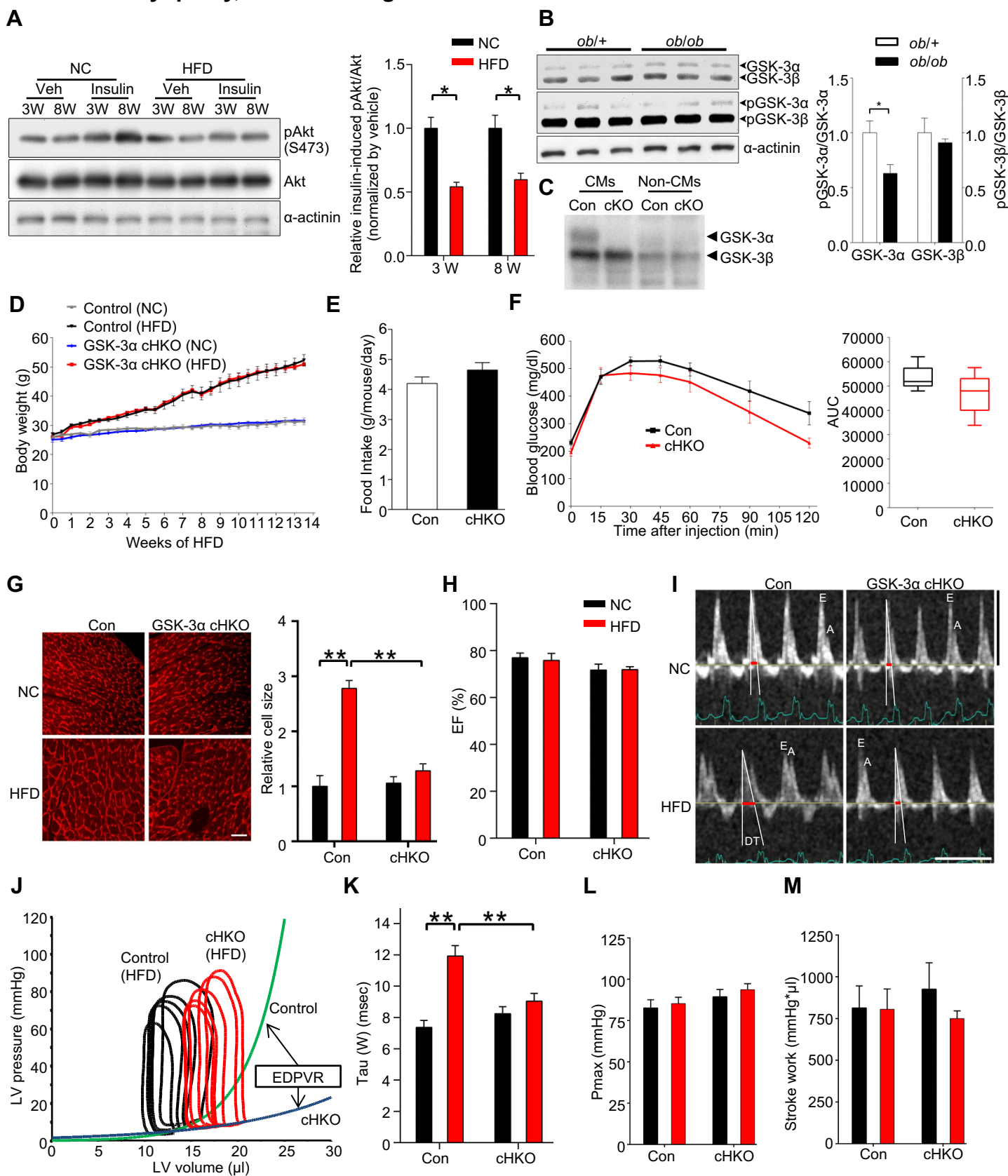


Figure S1. Knockdown of GSK-3 α attenuates high-fat diet (HFD)-induced lipotoxic cardiomyopathy, Related to Figure 1. (A) Immunoblots examining insulin resistance in the hearts of mice fed a HFD or normal chow (NC) for the indicated periods, as shown by insulin-stimulated phosphorylation of Akt (Ser473) (0.75 U/kg body weight, i.p.) (left). Quantification of insulin-induced pAkt normalized by Akt (n = 4) (right). (B) Immunoblots examining activities of GSK-3 α/β in the hearts of *ob/+* and *ob/ob* mice (left). Histograms show the ratios of phosphorylated versus total GSK-3 α/β (n = 6) (right). (C) Immunoblots showing the expression of GSK-3 α/β in cardiomyocytes (CMs) and non-myocytes (non-CMs) isolated from the hearts of GSK-3 α cardiac-specific homozygous knockout (cKO) or control homozygous floxed (Con) mice. (D to M) GSK-3 α cardiac-specific heterozygous knockout (cHKO) mice and heterozygous floxed (control) mice were fed a HFD or NC for 14 weeks. (D) Body weight growth curves (n = 5-7). (E) Food intake in mice fed a HFD (n = 10-12). (F) Intraperitoneal glucose tolerance test in HFD-fed control and GSK-3 α cHKO mice (left) and area under curve (n = 6) (right). (G) Wheat germ agglutinin staining of left ventricular (LV) cardiomyocyte cross sections. Scale bar, 100 μ m. Histograms show relative cardiomyocyte size, a marker of individual cardiomyocyte hypertrophy (n = 8) (right). (H) Echocardiographic analyses showing LV ejection fraction (EF, %) (n = 8 -15). (I) Representative images of transmitral flow obtained by Doppler echocardiography. Deceleration time (DT) is indicated by red bars. Transverse scale bar, 100 cm/s. Vertical scale bar, 100 ms. (J) Representative pressure-volume (PV) loop plots. Exponential curves show end-diastolic PV relation (EDPVR). (K to L) Tau, a marker of diastolic dysfunction (K), LV maximum pressure (L), and Stroke work (M), obtained by PV loop analysis (n = 5 for NC and n = 9 for HFD). Error bars indicate s.e.m. * $p < 0.05$, ** $p < 0.001$.

Figure S2. Knockdown of GSK-3 β exacerbates high-fat diet (HFD)-induced lipotoxic cardiomyopathy, Related to Figure 1.

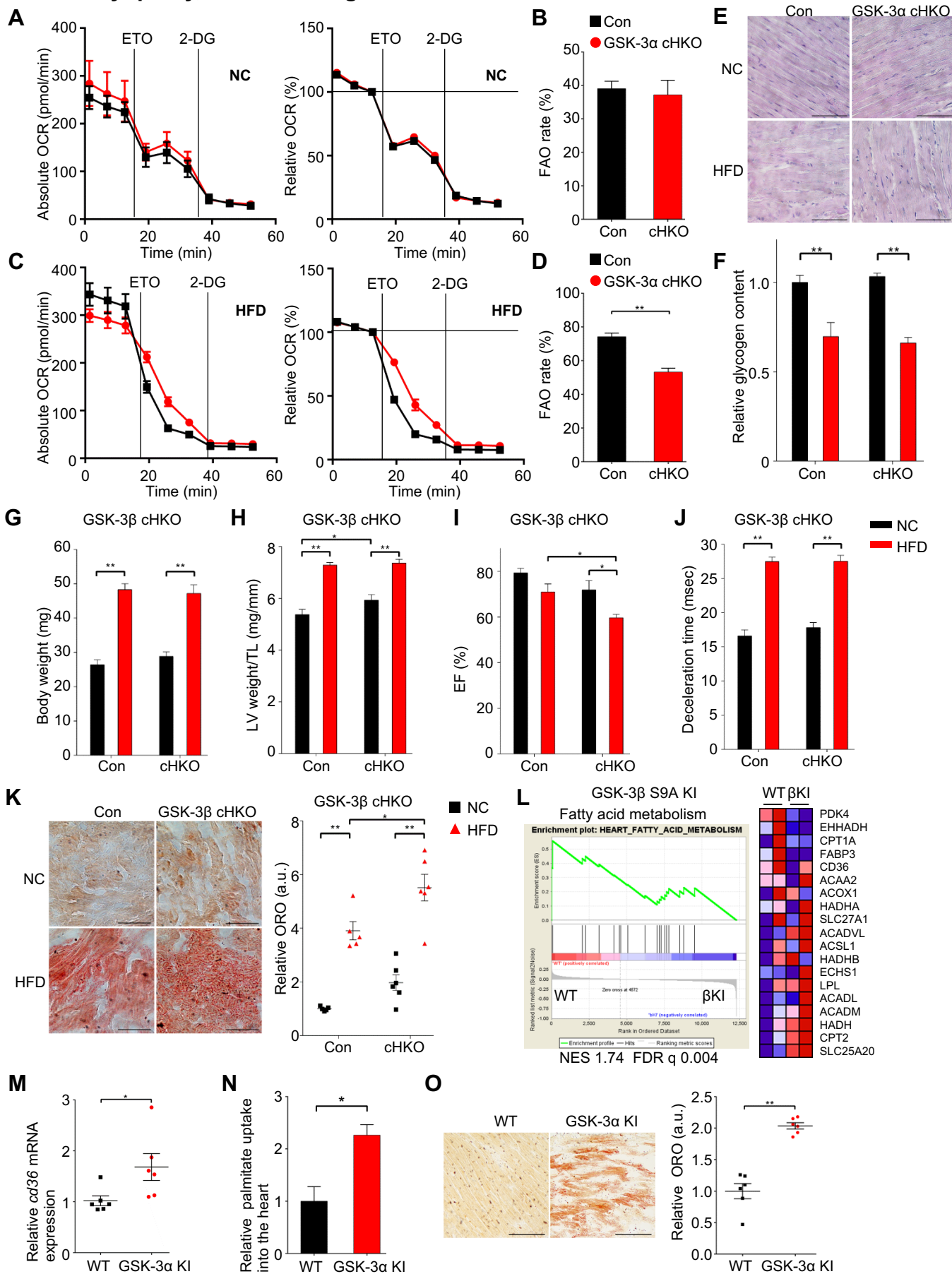


Figure S2. Knockdown of GSK-3 β exacerbates high-fat diet (HFD)-induced lipotoxic cardiomyopathy, Related to Figure 1. (A to D) Representative absolute and relative oxygen consumption rate (OCR) in CMs isolated from the hearts of GSK-3 α cHKO and control mice fed a HFD or normal chow (NC), measured by a Seahorse analyzer in the presence of 500 μ M of BSA-fatty acid cocktail (n = 3-4, A and C). Fatty acid oxidation (FAO) rate was evaluated by etomoxir (ETO)-inhibitable OCR. Histograms show FAO rate (the ratio of FAO versus OCR) (n = 4 (B, NC) and n = 8 (D, HFD)). (E and F) Representative Periodic acid-Schiff staining (E) and quantification of relative glycogen accumulation in the hearts of GSK-3 α cHKO and control mice fed a HFD or NC (n = 6) (F). Scale bar, 50 μ m. (G to K) GSK-3 β cardiac-specific heterozygous knockout (GSK-3 β cHKO) mice and heterozygous floxed (control) mice were fed a HFD or NC for 14 weeks. (G) Body weight after 14 weeks of the indicated diet (n = 5-6). (H) Left ventricular (LV) weight normalized by tibia length (TL), a marker of cardiac hypertrophy (n = 5-6). (I) Ejection fraction (EF), a marker of systolic function, obtained by M-mode echocardiography (n = 5-6). (J) Deceleration time, a marker of diastolic function, obtained by transmitral flow Doppler echocardiography (n = 5-6). (K) Representative Oil Red O staining of the indicated mouse heart sections (left), a marker of lipid accumulation. Scale bar, 25 μ m. Quantification of relative myocardial lipid accumulation (n = 5-6) (right). (L) Custom gene-set analysis representing enrichment of cardiac fatty acid metabolism in GSK-3 β Ser9Ala homozygous knock-in (KI) mouse hearts compared to wild-type (WT) mice at 3 months of age. (M to O) Fatty acid uptake and lipid accumulation were examined in the hearts of GSK-3 α S21A homozygous knockin (KI) and control wild-type (WT) mice fed NC (3 months of age). Relative *CD36* mRNA expression in the hearts (n = 6) (M), BSA-conjugated ³H-palmitate uptake into the hearts (n = 6) (N), and representative Oil Red O staining of the heart sections (left) and quantification of myocardial lipid accumulation (n = 6) (right). Scale bar, 50 μ m (O). Error bars indicate s.e.m. * $p < 0.05$, ** $p < 0.001$.

Figure S3. GSK-3 α , but not GSK-3 β , physically interacts with PPAR α , Related to Figure 2.

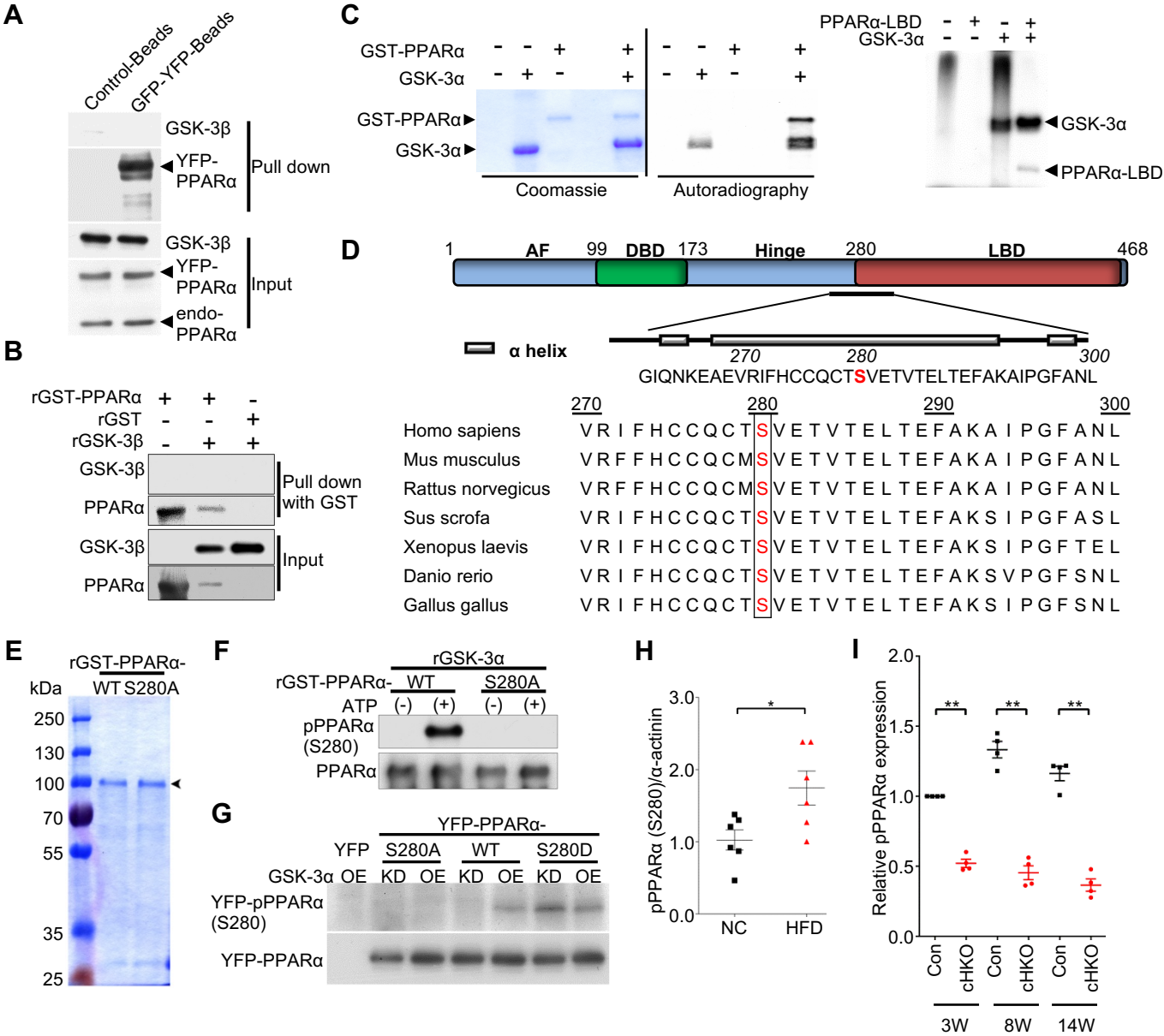


Figure S3. GSK-3 α , but not GSK-3 β , physically interacts with PPAR α , Related to Figure 2.

(A) Immunoprecipitation assays examining the interaction between endogenous GSK-3 β and YFP-tagged PPAR α in cardiomyocytes (CMs). Forty-eight hours after transduction with Ad-YFP-PPAR α , lysates were extracted for immunoprecipitation with anti-GFP-YFP antibody-conjugated or control beads, followed by immunoblotting with anti-GSK-3 β antibody. (B) *In vitro* binding assays examining direct interaction between recombinant (r) GSK-3 β and rGST-PPAR α . (C) *In vitro* kinase assays to test the ability of rGSK-3 α to phosphorylate rGST-PPAR α or rGST alone as a control (left). *In vitro* kinase assays to test the ability of rGSK-3 α to phosphorylate commercially available truncated rPPAR α protein, including the ligand binding domain (amino acids 170-430) (right). (D) Conservation of the PPAR α Ser280 phosphorylation site across species. (E) Coomassie Brilliant Blue staining of the rGST-PPAR α -wild type (WT) protein and phospho-resistant rPPAR α mutant protein with an alanine mutation of the Ser280 residue (rGST-PPAR α -S280A). (F) Immunoblots testing the sensitivity and specificity of the antibody against Ser280-phosphorylated PPAR α . An *in vitro* kinase assay was performed with active rGSK-3 α and rGST-PPAR α -WT or rGST-PPAR α -S280A mutant protein, followed by probing with the antibody against PPAR α -Ser280 phosphorylation. (G) Immunoblots showing Ser280 phosphorylation of PPAR α in CMs transduced with PPAR α -S280A, -WT, or -S280D or YFP alone as a control in the presence of adenovirus-mediated GSK-3 α overexpression (OE) or knockdown (KD) with palmitic acid treatment. (H) Histogram showing the ratio of Ser280-phosphorylated PPAR α versus α -actinin (n = 6). (I) Histogram showing relative expression of Ser280-phosphorylated PPAR α versus Histone H3 (n = 4). Error bars indicate s.e.m. * $p < 0.05$.

Figure S4. GSK-3 α -mediated Ser280 phosphorylation enhances PPAR α activity, Related to Figure 3.

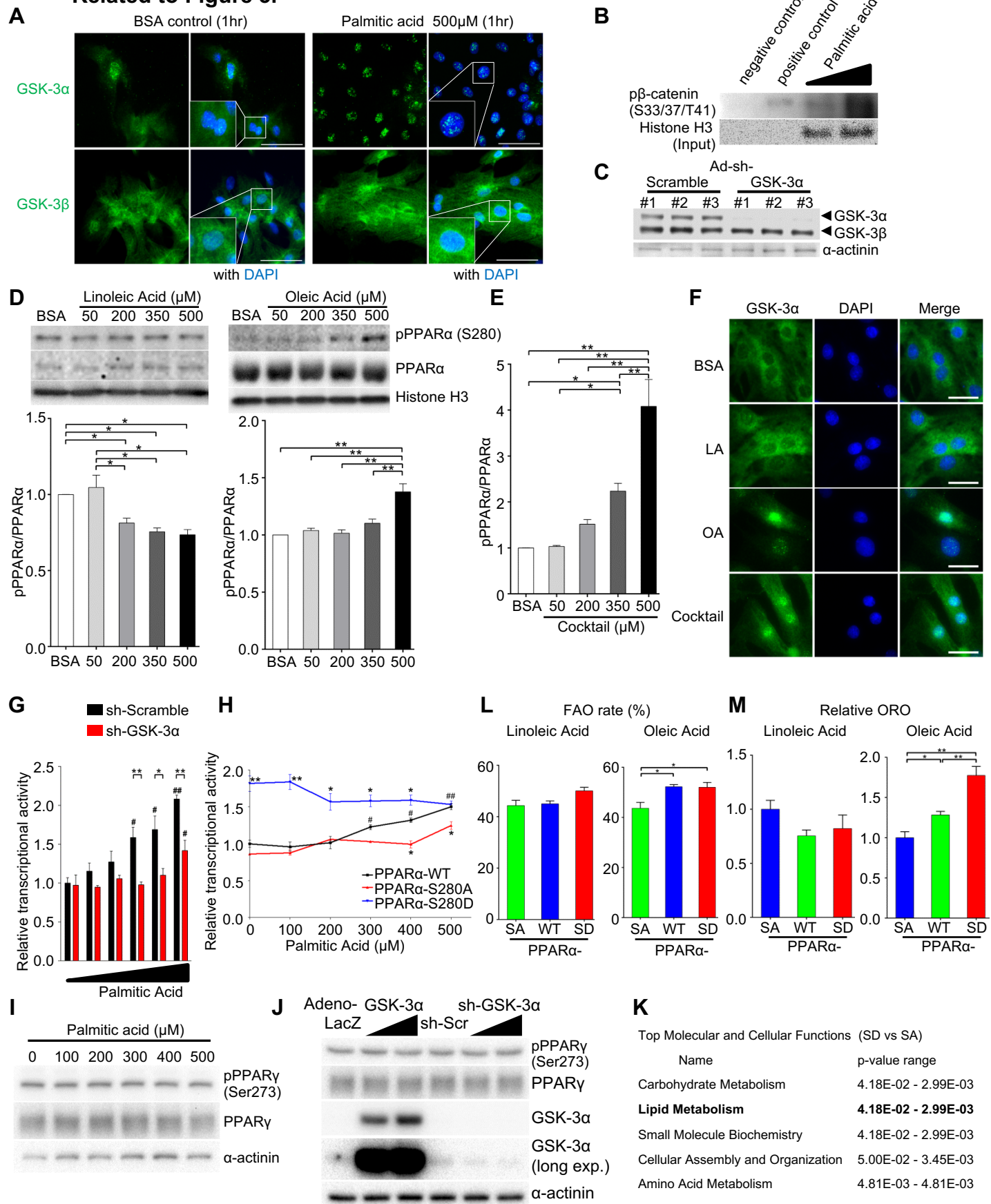


Figure S4. GSK-3 α -mediated Ser280 phosphorylation enhances PPAR α activity, Related to Figure 3. (A) Immunofluorescence staining for GSK-3 α (green, upper) or GSK-3 β (green, lower) and DAPI (blue) in primary cultured rat neonatal cardiomyocytes (CMs) treated with 500 μ M of BSA-conjugated palmitic acid (PA) or BSA control for 1 hour. Images are representative of three independent experiments. Scale bar, 50 μ m. (B) Immune complex *in vitro* kinase assays to examine nuclear GSK-3 α activity in CMs treated with PA. GSK-3 α was immunoprecipitated from the nuclear fraction of cultured CMs, followed by *in vitro* kinase assays with recombinant GST- β -catenin. Positive and negative control experiments were performed in the presence and absence of recombinant active GSK-3 α instead of CM lysate, respectively. (C) Immunoblots testing the efficiency of knockdown of GSK-3 α with adenovirus harboring shRNA-GSK-3 α or shRNA-scramble as a control, using anti-GSK-3 α / β antibody. (D and E) Immunoblots showing the expression of pPPAR α (Ser280) in the nucleus of CMs treated with BSA-linoleic acid (left) or BSA-oleic acid for 9 hours (right) and quantification analyses (n = 4) (D). Histogram showing the ratio of Ser280-phosphorylated PPAR α versus total PPAR α in the nucleus of CMs treated with BSA-fatty acid cocktail (n = 4) (E). (F) Immunofluorescence staining for GSK-3 α (green) and DAPI (blue) in CMs treated with 500 μ M of indicated BSA-conjugated fatty acid or BSA control for 1 hour. Images are representative of three independent experiments. Scale bar, 25 μ m. (G) The effect of GSK-3 α on the PA-induced increase in PPRE-luciferase reporter activity in CMs in the presence or absence of GSK-3 α knockdown (n = 8). # $p < 0.05$ and ## $p < 0.001$ compared to control (PA 0 μ M). (H) The effect of BSA-PA on PPRE-luciferase reporter activity in H9C2 cells transduced with PPAR α -WT, PPAR α -S280D or PPAR α -S280A mutant allele. YFP alone was used for background extraction (n = 4). * $p < 0.05$, ** $p < 0.001$ compared to PPAR α -WT. # $p < 0.05$, ## $p < 0.001$ compared to 0 μ M of PA in H9C2 cells with PPAR α -WT. One-way ANOVA Newman-Keuls post-hoc analysis. (I and J) Immunoblots showing the effect of PA (I) and GSK-3 α activity (J) on the phosphorylation of PPAR γ at Ser273 in CMs. (K) Ingenuity pathway analysis showing top 5 molecular and cellular functions in the PPAR α -SD versus the PPAR α -SA mutant. Gene expression was determined by RNA-seq data. (L) FAO rate in CMs treated with 500 μ M of BSA-linoleic acid (left) or BSA-oleic acid (right), measured by 96-well Seahorse analyzer (n = 7-8). (M) Relative lipid accumulation in CMs treated with 500 μ M of BSA-linoleic acid (left) or BSA-oleic acid (right) (n = 6). Error bars indicate s.e.m. * $p < 0.05$, ** $p < 0.001$.

Figure S5. PPAR α activity is increased by GSK-3 α -mediated Ser280-phosphorylation, Related to Figure 4.

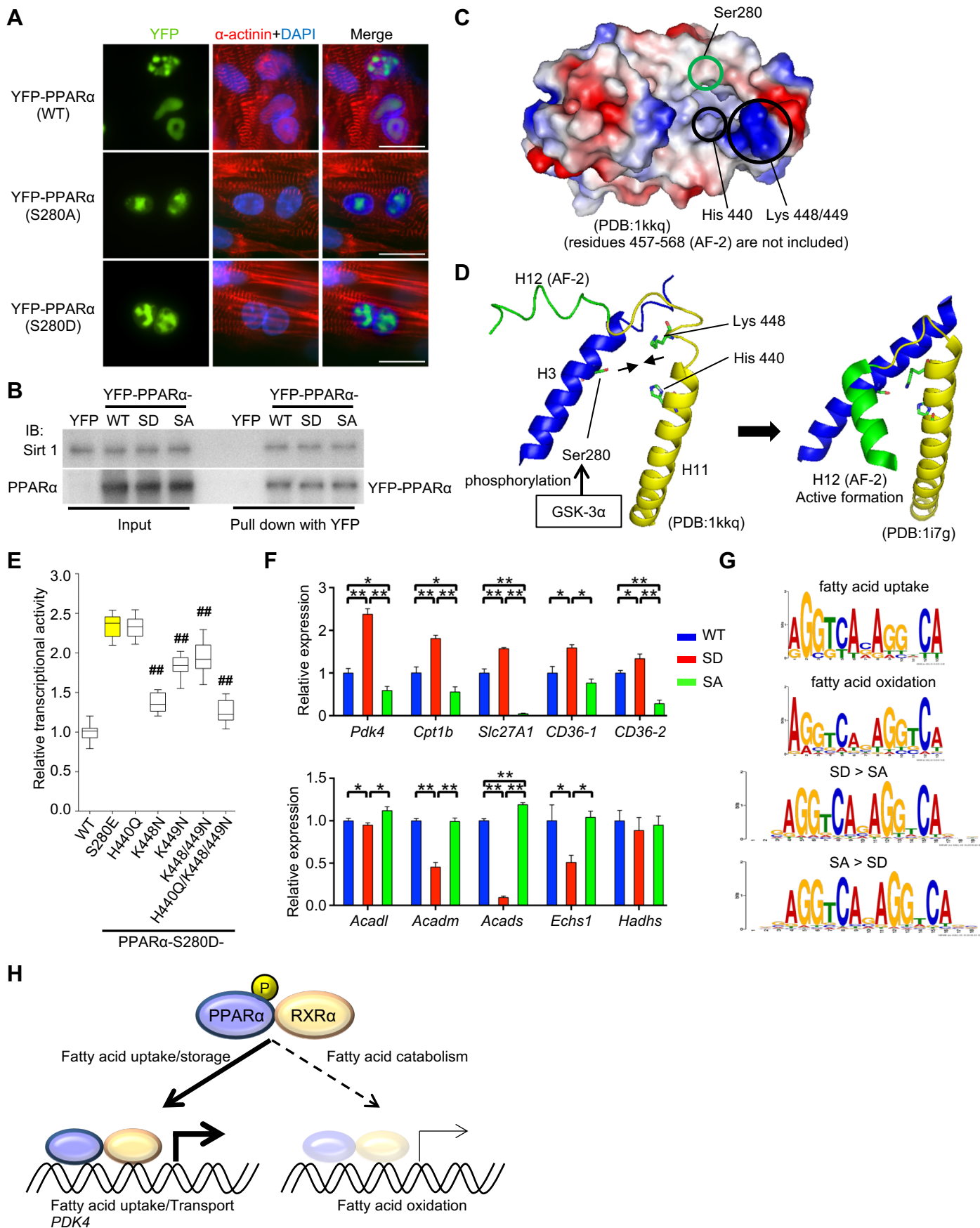


Figure S5. PPAR α activity is increased by GSK-3 α -mediated Ser280-phosphorylation, Related to Figure 4. (A) Immunofluorescence staining in cardiomyocytes (CMs) transduced with Ad-YFP-PPAR α -WT, -S280A or -S280D mutant for DAPI (blue) and α -sarcomeric actinin (red). Scale bar, 20 μ m. (B) Immunoprecipitation assays examining the interaction between Sirt1 and YFP-PPAR α -WT, -S280D, -S280A or YFP alone as a control in CMs. The data shown are representative of three independent experiments. (C) The surface of the PPAR α ligand binding domain (PDB: 1kkq), excluding residues 457-568. Red represents a negative charge and blue represents a positive charge. (D) A ribbon drawing of PPAR α helices 3, 11 and 12 (AF-2) (PDB: 1kkq and 1i7g). (E) PPRE-luciferase reporter activity in H9C2 cells transduced with PPAR α -WT, PPAR α -H440Q/K448N/K449N, PPAR α -S280E or PPAR α -S280D-H440Q/K448N/K449N mutant. YFP alone was used for background extraction (n = 12). ## $p < 0.001$ compared to PPAR α -S280E. (F) Quantification analyses of the ChIP assay normalized by the input level (n = 4). * $p < 0.05$, ** $p < 0.001$. (G) PPRE/DR1 (PPAR α -RXR α complex) sequence logos generated by the canonical PPRE/DR1 sequences enriched in the promoters of the genes related to fatty acid uptake or oxidation or the genes upregulated in PPAR α -S280D or PPAR α -S280A. (H) Schematic representation. S280-phosphorylated PPAR α preferentially binds to the promoters of genes for fatty acid uptake and *PDK4*, but not mitochondrial β -oxidation, thereby stimulating fatty acid uptake/storage. Error bars indicate s.e.m.

Figure S6. The development of lipotoxic cardiomyopathy is mediated by PPAR α -Ser280 phosphorylation, Related to Figure 5.

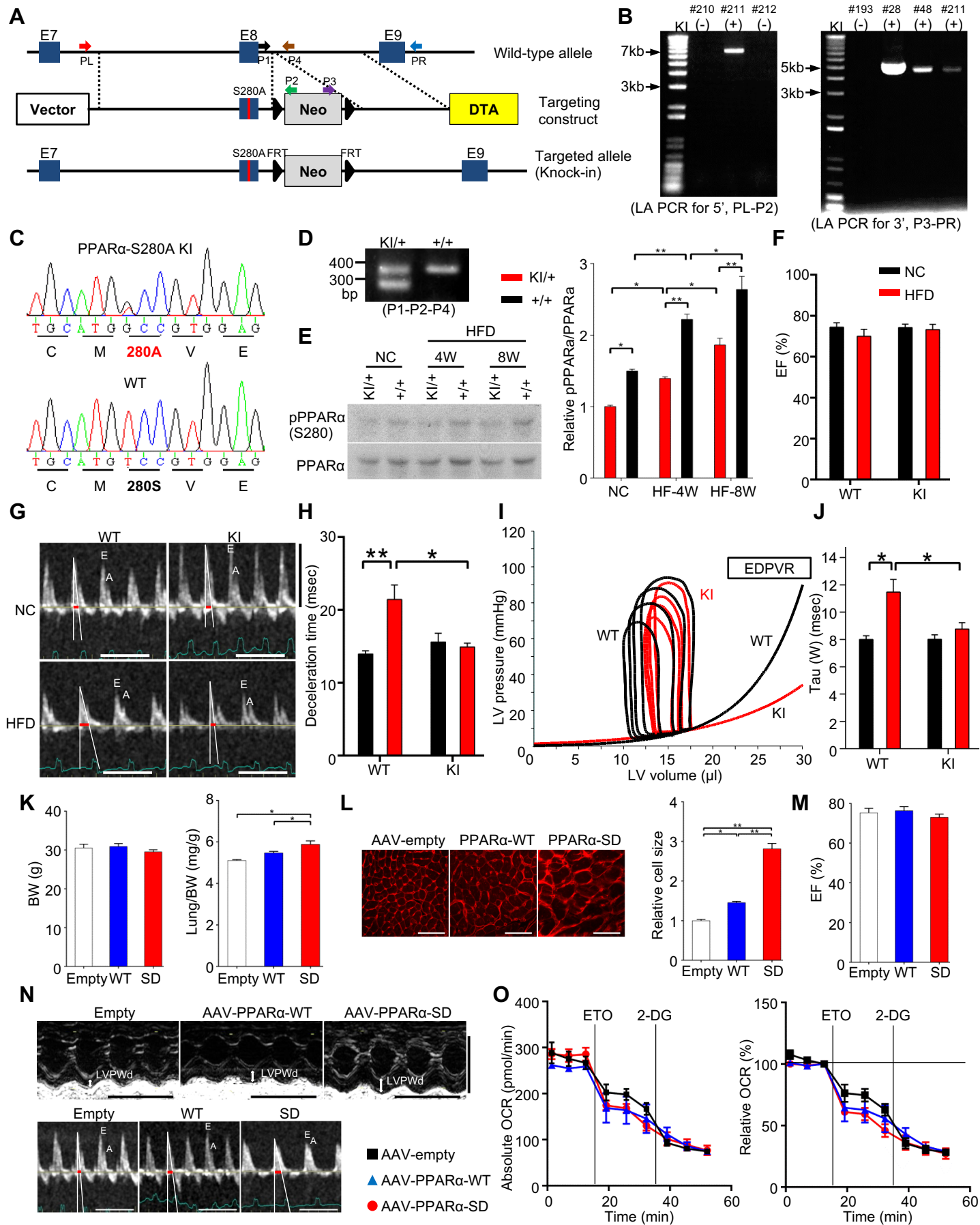


Figure S6. The development of lipotoxic cardiomyopathy is mediated by PPAR α -Ser280 phosphorylation, Related to Figure 5. (A) Schematic diagram of PPAR α -Ser280Ala knock-in (KI) gene targeting. The PPAR α genomic region of interest, the targeting construct, and the mutated Ser280Ala locus after homologous recombination are shown. P, PL and PR denote a primer, left primer, and right primer, used in (B) and (D). (B) DNA isolated from Neo-resistant ES clones was assessed by long range (LA) PCR for wild-type (WT) and heterozygous (het) alleles with the primers shown in (A). Positive ES clones identified by 5' LA-PCR were then verified by 3' LA-PCR. (C) Incorporation of Ser280Ala mutation into KI mice was verified by PCR and sequencing analyses using tail DNA. (D) PCR using tail DNA isolated from WT and heterozygous KI mice. Locations of the primers are shown in (A). (E to J) WT and S280A het KI mice were fed a high-fat diet (HFD) or normal chow (NC) for up to 8 weeks. (E) Immunoblots examining PPAR α -Ser280 phosphorylation in the heart (left). NC data was obtained from heart samples isolated from mice fed NC for 8 weeks. Quantification analyses of pPPAR α (Ser280) normalized by total PPAR α (n = 4) (right). (F) Echocardiographic analyses showing left ventricular (LV) ejection fraction (EF, %) (n = 6-7). (G) Representative images of transmitral flow obtained by Doppler echocardiography. Deceleration time is indicated by a red bar. Transverse scale bar, 100 cm/s. Vertical scale bar, 100 ms. (H) Deceleration time, evaluated by transmitral flow Doppler echocardiography (n = 6-7). (I) Representative pressure-volume (PV) loop plot for the indicated mice fed a HFD. Exponential curves show end-diastolic PV relation (EDPVR). (J) Tau, a marker of diastolic function, obtained by PV loop analysis (n = 5-8). (K to O) Either PPAR α -WT or PPAR α -S280D mutant was expressed in WT mouse hearts (C57BL/6J background) by adeno-associated virus (AAV)-mediated gene delivery and the mice were fed NC for 8 weeks. AAV-empty injection (Empty) was performed as a control. (K) Body weight (BW) (g) 8 weeks after AAV injections (left). Lung weight normalized by BW, a marker of congestive heart failure (n = 5-7) (right). (L) Wheat germ agglutinin staining of LV cardiomyocyte cross sections (left). Scale bar, 50 μ m. Histograms show relative cardiomyocyte size, a marker of individual cardiomyocyte hypertrophy (n = 4-6) (right). (M) LV ejection fraction (EF, %), evaluated by echocardiography (n = 5-6). (N) Representative images of M-mode echocardiogram (upper) and transmitral flow obtained by Doppler echocardiography (lower). Deceleration time is indicated by a red bar. (M-mode) Transverse scale bar, 100 ms. Vertical scale bar, 5 mm. (Doppler) Transverse scale bar, 100 cm/s. Vertical scale bar, 100 ms. (O) Representative absolute and relative oxygen consumption rate (OCR) of adult cardiomyocytes isolated from the hearts of mice transduced with the indicated AAV, measured by a 96-well Seahorse analyzer in the presence of 500 μ M of BSA-conjugated fatty acid cocktail (n = 3-4). Error bars indicate s.e.m. * $p < 0.05$, ** $p < 0.001$.

Figure S7. PPAR α ligands inhibit GSK-3 α -mediated PPAR α phosphorylation and ameliorate high-fat diet (HFD)-induced cardiac dysfunction, Related to Figure 6.

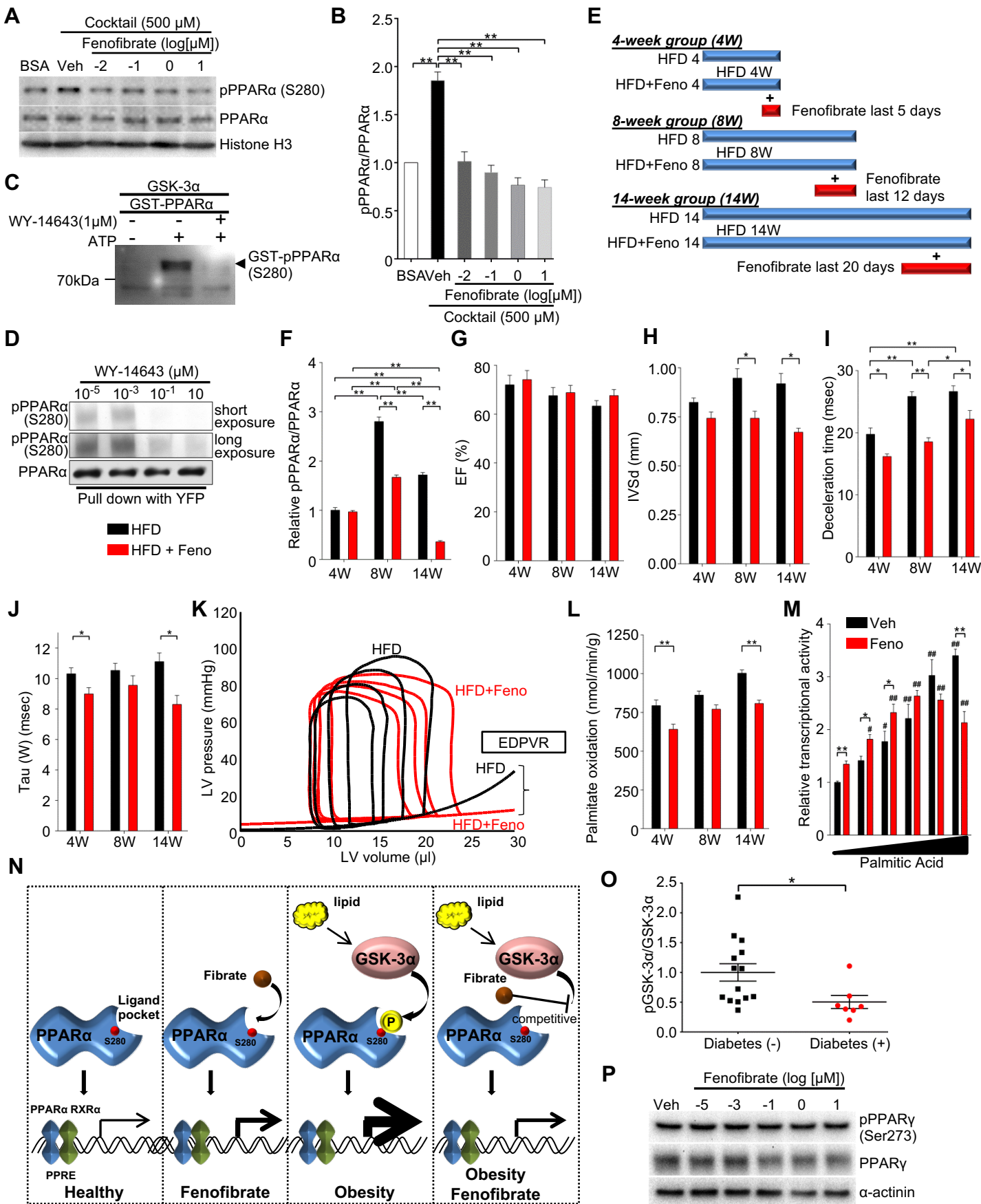


Figure S7. PPAR α ligands inhibit GSK-3 α -mediated PPAR α phosphorylation and ameliorate high-fat diet (HFD)-induced cardiac dysfunction, Related to Figure 6. (A and B) Immunoblots examining the effect of fenofibrate, a PPAR α ligand, on PPAR α -Ser280 phosphorylation in the nucleus of cardiomyocytes (CMs) in the presence of 500 μ M of BSA-fatty acid cocktail (A) and quantification analyses (n = 4) (B). (C) *In vitro* kinase assay using recombinant (r) GSK-3 α and rGST-PPAR α in the presence or absence of WY-14643 (1 μ M), a PPAR α ligand, followed by probing for Ser280-phosphorylated PPAR α . (D) The effect of WY-14643 on PPAR α -Ser280 phosphorylation in CMs. CMs were transduced with Ad-YFP-PPAR α and cultured with the indicated concentration of WY-14643, followed by immunoprecipitation with an anti-GFP-YFP antibody and probing for pPPAR α (Ser280). (E to L) Wild-type (WT) mice were fed a HFD in the presence or absence of fenofibrate for the indicated periods. (E) Schematic representation of HFD experiments with or without fenofibrate (Feno) for the indicated periods. (F) Quantification of the effect of fenofibrate on Ser280 phosphorylation of PPAR α shown in Figure 6B (n = 3). (G and H) Echocardiographic analyses of cardiac morphology and function. Ejection fraction (G, EF, %) and interventricular septal thickness at diastole (H, IVSd, mm) (n = 8-12). (I) Deceleration time, a marker of diastolic function, evaluated by transmitral flow Doppler echocardiography (n = 8-12). (J) Pressure-volume (PV) loop analyses to test diastolic function, as indicated by tau (n = 8-12). (K) Representative images showing PV loop. Exponential curves show end-diastolic PV relation (EDPVR). (L) Palmitate oxidation in the hearts (n = 16). (M) The effect of fenofibrate on PPRE-luciferase reporter activity in primary cultured rat neonatal CMs, depending on the concentration of BSA-palmitic acid (PA) (n = 8). # $p < 0.05$, ## $p < 0.001$ compared to 0 μ M of PA. (N) Schematic representation of fibrate- or lipid-induced PPAR α stimulation through activation of GSK-3 α and PPAR α -Ser280 phosphorylation in CMs. Fibrates inhibit GSK-3 α -mediated PPAR α phosphorylation by interfering with the interaction between GSK-3 α and PPAR α , thereby antagonizing lipid-induced activation of PPAR α and ameliorating cardiac lipotoxicity in obesity. (O) Histogram showing the ratio of phosphorylated versus total GSK-3 α (n = 7 with diabetes and n = 14 without diabetes). (P) Immunoblots showing the effect of fenofibrate on PPAR γ -Ser273 phosphorylation in CMs. Error bars indicate s.e.m. * $p < 0.05$, ** $p < 0.001$.

Table S1. Top 10 upregulated KEGG gene sets in wild-type (vs GSK-3 α knock-in) mouse heart, Related to Figure 1

	GS follow link to MSigDB	SIZE	ES	NES	NOM p-val	FDR q-val
1	KEGG_NEUROACTIVE_LIGAND_RECEPTOR_INTERACTION	221	-0.42	-2.27	0	0.001
2	KEGG_AUTOIMMUNE_THYROID_DISEASE	22	-0.66	-2.21	0	0.001
3	KEGG_ALLOGRAFT_REJECTION	16	-0.68	-2.19	0	0.001
4	KEGG_ASTHMA	15	-0.59	-1.84	0.01	0.019
5	KEGG_HEMATOPOIETIC_CELL_LINEAGE	66	-0.4	-1.81	0.005	0.019
6	KEGG_INTESTINAL_IMMUNE_NETWORK_FOR_IGA_PRODUCTION	31	-0.45	-1.73	0.008	0.028
7	KEGG_JAK_STAT_SIGNALING_PATHWAY	125	-0.31	-1.6	0	0.062
8	KEGG_PRIMARY_IMMUNODEFICIENCY	33	-0.42	-1.6	0.016	0.055
9	KEGG_CYTOKINE_CYTOKINE_RECEPTOR_INTERACTION	201	-0.29	-1.53	0	0.077
10	KEGG_CELL_ADHESION_MOLECULES_CAMS	103	-0.31	-1.52	0	0.074

Table S2. Upregulated KEGG gene sets in PPAR α -S280D vs in PPAR α -WT (FDR q<0.25), Related to Figure 3

	GS follow link to MSigDB	SIZE	ES	NES	NOM p-val	FDR q-val
1	KEGG_RETINOL_METABOLISM	28	0.69	1.84	0	0.03
2	KEGG_TYPE_I_DIABETES_MELLITUS	20	0.71	1.79	0	0.03
3	KEGG_TERPENOID_BACKBONE_BIOSYNTHESIS	15	0.75	1.74	0	0.04
4	KEGG_FATTY_ACID_METABOLISM	33	0.61	1.69	0.003	0.06
5	KEGG_GLYCEROLIPID_METABOLISM	43	0.57	1.67	0.002	0.07
6	KEGG_GAP_JUNCTION	69	0.53	1.64	0.001	0.08
7	KEGG_LONG_TERM_POTENTIATION	64	0.51	1.6	0.003	0.11
8	KEGG_ALLOGRAFT_REJECTION	15	0.68	1.57	0.02	0.13
9	KEGG_BLADDER_CANCER	39	0.52	1.51	0.024	0.21
10	KEGG_GNRH_SIGNALING_PATHWAY	92	0.46	1.5	0.013	0.2
11	KEGG_TASTE_TRANSDUCTION	26	0.57	1.5	0.026	0.2
12	KEGG_STARCH_AND_SUCROSE_METABOLISM	33	0.53	1.48	0.034	0.2
13	KEGG_TRYPTOPHAN_METABOLISM	37	0.52	1.46	0.03	0.23
14	KEGG_CALCIIUM_SIGNALING_PATHWAY	165	0.41	1.46	0.004	0.22

Table S3. Myocardial metabolites in the heart of wild-type and PPAR α -S280A knock-in mice, Related to Figure 5.

PATHWAY		METABOLITE	Mean \pm SEM		FOLD CHANGE	p-value		
			WT	KI				
TCA cycle		citric acid	29.9 \pm 3.0	22.2 \pm 2.5	0.742	0.056		
		isocitric acid	11.7 \pm 1.6	9.1 \pm 0.9	0.777	0.148		
		succinic acid	177.9 \pm 24.0	228.3 \pm 69.3	1.283	0.465		
		fumaric acid	152.2 \pm 19.9	75.9 \pm 11.0	0.499	0.006		
		malic acid	256.0 \pm 38.1	119.3 \pm 20.1	0.466	0.008		
Glucose metabolism		Glycolysis		glucose-1-phosphate	10.7 \pm 2.1	9.7 \pm 1.6	0.905	0.676
				glucose-6-phosphate	72.0 \pm 15.3	59.3 \pm 11.1	0.824	0.475
				fructose-6-phosphate	75.8 \pm 14.5	66.0 \pm 11.7	0.870	0.572
				Glycerol 3-phosphate	199.7 \pm 31.9	290.4 \pm 119.4	1.455	0.436
				3-phosphoglycerate	16.9 \pm 3.6	12.6 \pm 2.7	0.748	0.322
				pyruvic acid	8.6 \pm 0.6	7.9 \pm 0.8	0.918	0.431
				lactic acid	447.5 \pm 142.1	999.1 \pm 629.3	2.233	0.367
		Myoinositol	41.8 \pm 2.9	31.5 \pm 5.6	0.754	0.106		
		myo-inositol 1-phosphate	60.9 \pm 4.4	44.2 \pm 13.3	0.725	0.217		
Fatty acid metabolism		Saturated FFA		12:0	5.1 \pm 0.7	4.1 \pm 0.6	0.803	0.266
				14:0	16.4 \pm 0.8	14.5 \pm 2.0	0.887	0.362
				16:0	2163.4 \pm 102.5	1515.3 \pm 234.5	0.700	0.022
				17:0	16.6 \pm 0.5	12.2 \pm 2.5	0.734	0.094
				18:0	3786.7 \pm 233.9	2538.3 \pm 600.0	0.670	0.062
		Unsaturated FFA		19:0	8.3 \pm 0.4	5.7 \pm 1.5	0.683	0.100
				16:1	4.5 \pm 0.4	2.8 \pm 0.5	0.616	0.017
				18:2	249.3 \pm 11.1	175.1 \pm 45.6	0.702	0.115
				18:1	124.3 \pm 5.9	82.5 \pm 20.8	0.664	0.063
				18:1 (trans)	45.6 \pm 1.2	29.9 \pm 8.9	0.656	0.085
				20:4	123.7 \pm 4.6	76.0 \pm 28.0	0.614	0.096
					1-Linoleoyl-glycerol	24.3 \pm 0.6	17.6 \pm 3.3	0.723
				1-Oleoyl-glycerol	24.8 \pm 1.1	16.8 \pm 3.7	0.678	0.050
				1-monostearoylglycerol	402.6 \pm 22.9	351.2 \pm 29.5	0.872	0.163
				1-monopalmitoylglycerol	295.8 \pm 23.0	240.2 \pm 14.4	0.812	0.051
				2-monooleoylglycerol	12.4 \pm 0.3	9.1 \pm 1.8	0.732	0.075
				glycerol	152.5 \pm 6.9	132.3 \pm 10.8	0.867	0.115
cholesterol	2328.9 \pm 124.7			1875.4 \pm 114.0	0.805	0.017		
Amino acid metabolism		BCAA		valine	310.0 \pm 28.3	333.7 \pm 90.4	1.076	0.787
				leucine	230.6 \pm 29.0	264.7 \pm 75.7	1.148	0.651
				isoleucine	113.6 \pm 13.4	132.0 \pm 37.6	1.163	0.619
				alanine	71.6 \pm 7.6	66.4 \pm 10.0	0.928	0.658
				aspartic acid	5578.5 \pm 874.2	3928.1 \pm 1207.1	0.704	0.251
				asparagine	30.0 \pm 2.6	21.0 \pm 2.9	0.701	0.033
				cysteine	7.9 \pm 0.5	6.9 \pm 1.0	0.866	0.326
				L-Glutamic acid	470.9 \pm 104.4	424.0 \pm 104.6	0.900	0.732
				glutamine	2105.4 \pm 177.2	2001.0 \pm 256.2	0.950	0.718
				glycine	32.7 \pm 3.1	29.3 \pm 1.3	0.896	0.288
				histidine	14.7 \pm 1.9	8.5 \pm 0.6	0.580	0.009
				lysine	161.6 \pm 24.6	94.5 \pm 6.0	0.585	0.018
				L-Methionine	89.0 \pm 11.3	66.2 \pm 8.2	0.744	0.105
				proline	2.3 \pm 0.4	2.3 \pm 0.4	0.993	0.975
				phenylalanine	63.7 \pm 4.8	65.6 \pm 5.2	1.029	0.782
				serine	738.2 \pm 78.4	494.5 \pm 50.5	0.670	0.019
				tyrosine	17.9 \pm 4.3	17.2 \pm 2.5	0.964	0.890
				tryptophan	49.4 \pm 7.9	26.9 \pm 3.6	0.544	0.020
				2-aminoadipic acid	2.8 \pm 0.6	1.4 \pm 0.3	0.505	0.039
				threonine	85.4 \pm 13.2	54.7 \pm 5.9	0.640	0.045
				homoserine	6.1 \pm 0.5	6.2 \pm 0.9	1.011	0.942
				glycolic acid	15.0 \pm 0.9	12.0 \pm 1.0	0.799	0.041
				glyceric acid	7.6 \pm 0.3	7.1 \pm 0.6	0.934	0.436
				2-hydroxyglutarate	6.3 \pm 0.7	8.2 \pm 2.1	1.309	0.349
		homocysteine	1.6 \pm 0.2	1.4 \pm 0.1	0.836	0.152		
		N-methylalanine	32.5 \pm 5.0	16.3 \pm 2.9	0.502	0.014		
		sarcosine	8.8 \pm 2.3	5.0 \pm 0.8	0.568	0.122		
		Urea cycle		ornithine	18.8 \pm 5.4	14.2 \pm 1.1	0.753	0.377
				urea	131.1 \pm 10.0	129.6 \pm 11.7	0.989	0.915
				N-acetylaspartate	1.5 \pm 0.4	1.1 \pm 0.1	0.716	0.310
				B-alanine	1.7 \pm 0.4	1.4 \pm 0.2	0.871	0.617
		inorganic phosphate		phosphate	11701.2 \pm 926.0	11833.7 \pm 708.6	1.011	0.902
diphosphate	271.6 \pm 48.5			177.0 \pm 53.3	0.651	0.180		
Purine/primidine metabolism		Adnine nucleotides		hypoxanthine	5.4 \pm 3.2	5.3 \pm 2.1	0.977	0.972
				adenosine	75.4 \pm 13.3	60.2 \pm 8.0	0.798	0.306
				inosine	5.0 \pm 2.2	3.4 \pm 1.2	0.686	0.513
				adenine	10.7 \pm 0.6	9.1 \pm 0.8	0.845	0.096
				5'-Adenosine monophosphate	1148.3 \pm 210.8	824.1 \pm 191.5	0.718	0.239
				uric acid	2.3 \pm 0.7	1.4 \pm 0.3	0.593	0.184
				uracil	0.9 \pm 0.3	1.3 \pm 0.6	1.477	0.536
Others		creatinine	1640.6 \pm 68.9	1175.0 \pm 53.2	0.716	0.000		
		pantothenic acid	29.7 \pm 3.9	17.0 \pm 2.7	0.572	0.017		
		3-hydroxybutyrate	12.7 \pm 8.4	13.2 \pm 5.8	1.036	0.961		
		nicotinamide	88.5 \pm 4.1	70.8 \pm 6.3	0.799	0.030		
		glutathione	36.0 \pm 2.1	23.0 \pm 2.6	0.639	0.002		
		2,4-dihydroxybutanoic acid	52.7 \pm 2.1	42.7 \pm 4.2	0.810	0.044		
		serotonin	4.7 \pm 0.5	4.9 \pm 2.1	1.050	0.904		
		dopamine	2.7 \pm 0.4	1.4 \pm 0.4	0.530	0.039		
		1,3-bisphosphoglycerate	1.3 \pm 0.1	0.9 \pm 0.2	0.686	0.090		
		2-hydroxybutyric acid	25.7 \pm 3.4	14.8 \pm 1.8	0.576	0.014		
		kynurenine	0.4 \pm 0.0	0.3 \pm 0.1	0.617	0.063		
		gluconic acid	15.7 \pm 1.8	10.7 \pm 1.5	0.687	0.049		
		ribitol	1.6 \pm 0.2	1.1 \pm 0.1	0.674	0.057		
		phosphoethanolamine	8.4 \pm 0.3	8.0 \pm 0.7	0.949	0.533		


 Decreased metabolite (p<0.05)

Table S4. Information on human heart samples, Related to Figure 6.

	Diabetes (-) (n = 14)	Diabetes (+) (n = 7)	P value
Age (year)	52.0 ± 11.8	50.4 ± 11.6	0.776
Male (n)	13 (92.9%)	6 (85.7%)	1.000
Hypertension (n)	5 (35.7%)	4 (57.1%)	0.397
Body weight (kg)	68.4 ± 2.4	71.4 ± 4.8	0.540
Height (cm)	168.2 ± 2.1	165.2 ± 2.6	0.409
Body mass index (kg/m ²)	24.3 ± 0.9	26.0 ± 1.2	0.259

Table S5. Oligonucleotide used in this paper, Related to STAR Methods

Name	Forward Primer	Reverse Primer
(A) qPCR Primers		
(mouse)		
Cd36	CCTCCAGAATCCAGACAACC	CACAGGCTTTCCTTCTTTGC
Slc27a1	ATCTACGGGTTGACGGTGGTA	GGTAGCGGCAGATTTACCTA
Lpl	AGAGAGGACTCGGAGACGTG	GGAGTTGCACCTGTATGCCT
Cpt1b	TGGCTGAGGTACTTTCTGAACC	AGAGACCCCGTAGCCATCAT
Acadm	GCTAGTGGAGCACCAAGGAG	CCAGGCTGCTCTCTGGTAAC
Acadl	TTCCGGGAGAGTGTAAAGGA	ACTTCTCCAGCTTCTCCCA
Acadvl	GCTCTGCAAGGCTGTATGGA	CGATTCTGTCTCCCGTCTC
Echs1	CCAGTTCGGACAGCCAGAAA	ACAAGACTGCCTGCTTTGC
Pdk4	TGACTCAAAGACGGGAAACC	ACTGGTCGCAGAGCATCTT
Glut4	TTGGGAAGGAAAAGGGCTAT	GAGGAACCGTCCAAGAATGA
Adiponectin	CTCCACCCAAGGGAACCTGT	AGGACCAAGAAGACCTGCATC
Adipsin	CGTACCATGACGGGGTAGTC	GAGTCTCCCCTGCAAGTGTC
Leptin	ACATTTACACACGCAGTCG	ACTCAGAATGGGGTGAAGCC
IL-6	CCGGAGAGGAGACTTCACAG	TGCCATTGCACAACCTTTTT
TNF α	CCCTCACACTCAGATCATCTTCT	GCTACGACGTGGGCTACAG
Pgc1 α	TCACACCAAACCCACAGAAA	TCTGGGGTCAGAGGAAGAGA
Ppara	ATGCAGTACTGCCGTTTTTC	CCGAATCTTTCAGGTCGTGT
Ppar δ	GACAATCCGCATGAAGCTC	CAAAGCGGATACGCTGTGTG
Ppar γ	TTCAGAAGTGCCTTGCTGTG	CCAACAGCTTCTCCTTCTCG
(Rat)		
Cd36	TTCAAGGTGTGCTCAACAGC	CCCCACAAGAGTTTCTTCAA
Slc27a1	TGAGAAGCGCCTAGGACTTTG	TCCGCATCCTTCTCTGGCTTG
Lpl	CCATGGATGGACGGTGACAG	ATAATGTTGCTGGGCCCGAT
Cpt1b	CCATCATGGTGAACAGCAAC	CTCTTCTCGGTCCAGTTTGC
Acadl	GGTTTCAGCCTCCATTCAGA	TCATCTGGGGGATAAACTGC
Acadm	GTCGCCCCAGACTACGATAA	GCCAAGACCACCACAACCTCT
Acadvl	AAGCCAGAGACCCTCTCCTC	CAGATGGGTATGGGAACACC
Echs1	CTCGCTGTTGTCCCCAGTTC	TTCAACTGGATCAGCCCCAC
Hadhb	CGCATCCTTCGCAGACTCTA	TGGGGCAGACTGTACTTGTG
Pdk4	CAAGAATTGCCCGTCAGACT	GACGGAAGGGGTGTCACTA
Atp5b	ACCACCAAGAAGGGCTCGAT	CCCAACTCAGCAATAGCACG
Atp5d	GGCCTGGACAGATGTCCTTC	CAAAGGTCAGGTCAGCGTA
Atp5g1	CTGACGGGGAGTGGGAGT	TACTCAGGAGGGAGGCAGAC
Ndufb6	GTACCGCACCCAGTCTCTCAC	TTCTGGGCTTCGTGCCAAC
Pgc1 α	CAGAACCATGCAAACCACAC	TTGTGGCTTTTGTGTTGAC
(B) ChIP primers (rat)		
Pdk4	TGTAACAAGGACAAGTCTGGGCG	AAGGGGCAAAGGGTGAGAGGGA
Cpt1b	CAGACCCATACCCGACAGA	CGGCTGAGAGTAAGGGTGAA
Slc27A1	TGAGAAGCGCCTAGGACTTT	ATGCTGACCTTCTCTGGCTT
Cd36-1	CAGTTCTAAGATCATGGACCCC	TGTTGCCCTGCAGATCAAAC
Cd36-2	GCGTGCATAGCAAACCAA	TGTGGCCTGGTTCAACTATT
Acadl	GACTGACCCTGGACTCTGAC	CCGCAACAATCACGTTCACT
Acadm	TTAGCCGCTCCAGTGTACAC	ATACCGGGGAAAGCTGGAC
Acads	TGCCATCCGGAACCTTAGAG	GATCTCCGCCCTGTGACC
Echs1	TACTCAAAGAACCGCCGCTA	GGAGACGGAAGCTAAAGGGA
Hadhs	TCTCTGGGAAGCAGCTAATGT	AGAATGGCAAATAGGGAATTGGT
(C) Primers for oligo pull-down		
Cd36	AAAGCAAGGTAAAAGGTCAAGGGCA	TGCCCTTGACCTTTTACCTTGCTTT
Slc27A1	AGTGGGGCAAAGGGCACAGGAGATG	CATCTCCTGTGCCCTTTGCCCACT
Acadm	GGCACAAGCTCAGAGGTCAGTAAAT	ATTTACTGACCTCTGAGCTTGTGCC
Echs1	CCGCTCAGGTCACGGGTCCACCCCT	AGGGGTGGACCCGTGACCTGAGCGG
(D) Primers for recombinant proteins, adenovirus, and site-directed mutagenesis		
GST-PPAR α -T1	ATTGGATCCGTGGACACAGAGAGCCCCA	ATTATTGTCGACTCACATGCACTGGCAGCAGTG
GST-PPAR α -T2	ATTGGATCCGTGGACACAGAGAGCCCCA	ATTATTGTCGACTCACAGGCACTTGTGAAAAACGG
GST-PPAR α -T3	ATTGGATCCGTGGACACAGAGAGCCCCA	ATTATTGTCGACTCAGATGTTTACAGGGCACTGCC
GST-PPAR α -T4	ATTGGATCCGTGGACACAGAGAGCCCCA	ATTATTGTCGACTCAGTCTGTGATGACAGAGCCCTC
GST-PPAR α -T5	ATGGATCCACCTCTCTCCAGCTTCCAG	ATTATTGTCGACTCAGTACATGTCTCTGTAGATCTCTGC
GST- β -catenin	ATTATTGGTACCGTACTCAAGCTGATTTGATGAGT	ATTATTAGGATCCTTACAGGTGAGTATCAAACCAGGC
PPAR α -S280A	CCAGTGCATGGCCGTGGAGACCG	CGGTCTCCACGGCCATGCACTGG
PPAR α -S280D	CCAGTGCATGGACGTGGAGACCG	CGGTCTCCACGTCCATGCACTGG
PPAR α -S280E	CCAGTGCATGGAGGTGGAGACCG	CGGTCTCCACCTCCATGCACTGG

PPAR α -H440A	GGTCACGGAGGCTGCGCAGCTCG	CGAGCTGCGCAGCCTCCGTGACC
PPAR α -H440Q	GTACACGGAGCAAGCGCAGCTCG	CGAGCTGCGCTTGCTCCGTGAC
PPAR α -K448A	CGTACAGGTCATCGCGAAGACCGAGTCCG	CGGACTCGGTCTTCGCGATGACCTGTACG
PPAR α -K449A	CAGGTCATCAAGGCGACCGAGTCCGACG	CGTCGGACTCGGTTCGCCTTGATGACCTG
PPAR α -K448/449A	CGTACAGGTCATCGCGGCGACCGAGTCCGAC	GTCGGACTCGGTTCGCCGCGATGACCTGTACG
PPAR α -K448N	CGTACAGGTCATCAACAAGACCGAGTCCG	CGGACTCGGTCTTGTTGATGACCTGTACG
PPAR α -K449N	CAGGTCATCAAGAACACCGAGTCCGACG	CGTCGGACTCGGTGTTCTTGATGACCTG
PPAR α -K448/449N	CGTACAGGTCATCAACAACACCGAGTCCGAC	GTCGGACTCGGTGTTGTTGATGACCTGTACG
pDC-YFP- PPAR α	ATTCCCGGGGTGGACACAGAGAGCCCC	ATTATTGTCGACTCAGTACATGTCTCTGTAGATCTCT TG
(E) Primers for mouse generation and genotyping		
Subcloning, long arm	ATTATTGGATCCGGCGCGCCTATCAGCTCCCCT GGAAGTAAA	ATTAGATATCCTCACTCAGTTCCACTCCACAG
Subcloning, short arm	ACTAACTGTCGACGCGGCCGCCTGTGGAGTGG AACTGAGTGAGAACAGTAT	ATTATCTCGAGACCGCCTCTGATGGGTACAGACA
5' Selection (PL-P2)	ACCTGAGCTTGATCCTTGC	TGGGTCGTTTGTTCGGATCT
3' Selection (P3-PR)	TCCAGACTGCCTTGGGAAAA	GGGAAGGTCAGTAAGGGTGC
PPAR α -KI (P1-P2)	AGTGGATCTGTCACTCGCAG	TGGGTCGTTTGTTCGGATCT
PPAR α -KI (P1-P4)	AGTGGATCTGTCACTCGCAG	AGCACTGCACCTAAACCTGC
α MHC-Cre	ATGACAGACAGATCCCTCCTATCTCC	CTCATCACTCGTTGCATCGAC
GSK-3 α floxed	CCAACCCTCCAGTCCTTATC	CAGGCTACCCAGCCTTTC
GSK-3 β floxed-Neo	GGGAGGATTGGGAAGACAAT	ACAATGTGCCGAGTTCATCA
GSK-3 β floxed-WT	TTGGCAATTTGAAAGGGAAG	ACAATGTGCCGAGTTCATCA
GSK-3 α KI	TTGAAGTGGCTGGTACTGGCTCTG	GTGTGCTCCAGAGTAGTACCTAGC
GSK-3 β KI	TCACTGGTCTAGGGGTGGTGGAAAG	GGAGTCAGTGACAACACTTAACTT
(F) shRNA targeting sequence (rat)		
GSK-3 α #1	GTGATTGGCAATGGCTCAT	
GSK-3 α #2	GGTGTCAAATCTCGGACA	
GSK-3 α #3	GCTTTAACTGAGACTCAGA	